Biochemical and Biophysical Research Communications 423 (2012) 373–378

Contents lists available at SciVerse ScienceDirect

Biochemical and Biophysical Research Communications

journal homepage: www.elsevier.com/locate/ybbrc

Dissecting the role of disulfide bonds on the amyloid formation of insulin

Yang Li [a], Hao Gong [a], Yue Sun [b], Juan Yan [a], Biao Cheng [a], Xin Zhang [a], Jing Huang [b], Mengying Yu [a], Yu Guo [a], Ling Zheng [b,*], Kun Huang [a,c,*]

[a] Tongji School of Pharmacy, Huazhong University of Science and Technology, Wuhan 430030, PR China
[b] College of Life Sciences, Wuhan University, Wuhan 430072, PR China
[c] Centre for Biomedicine Research, Wuhan Institutes of Biotechnology, Wuhan 430070, PR China

ARTICLE INFO

Article history:
Received 18 May 2012
Available online 1 June 2012

Keywords:
Insulin
Diabetes
Disulfide bonds
Fibrillation
Oligomerization
Hemolysis

ABSTRACT

Disulfide bonds play a critical role in the stability and folding of proteins. Here, we used insulin as a model system, to investigate the role of its individual disulfide bond during the amyloid formation of insulin. Tris(2-carboxyethyl)phosphine (TCEP) was applied to reduce two of the three disulfide bonds in porcine insulin and the reduced disulfide bonds were then alkylated by iodoacetamide. Three disulfide bond-modified insulin analogs, INS-2 (lack of A6-A11), INS-3 (lack of A7-B7) and INS-6 (lack of both A6-A11 and A7-B7), were obtained. Far-UV circular dichroism (CD) spectroscopy results indicated that the secondary structure of INS-2 was the closest to insulin under neutral conditions, followed by INS-3 and INS-6, whereas in an acidic solution all analogs were essentially unfolded. To test how these modifications affect the amyloidogenecity of insulin, thioflavin-T (ThT) fluorescence and transmission electronic microscopy (TEM) were performed. Our results showed that all analogs were more prone to aggregation than insulin, with the order of aggregation rates being INS-6 > INS-3 > INS-2. Cross-linking of unmodified proteins (PICUP) assay results showed that analogs without A6-A11 (INS-2 and INS-6) have a higher potential for oligomerization than insulin and INS-3, which is accompanied with a higher cytotoxicity as the hemolytic assays of human erythrocytes suggested. The results indicated that breakage of A7-B7 induced more unfolding of the insulin structure and a higher amyloidogenicity than breakage of A6-A11, but breakage of A6-A11 caused a significant cytotoxicity increase and a higher potency to form high order toxic oligomers.

1. Introduction

It is generally accepted that most proteins are potentially able to misfold into amyloid under appropriate conditions [1]. Protein fibrillation was associated with amyloidogenic diseases like Alzheimer's Disease and Parkinson's Disease. Protein fibrillation may be influenced by disulfide bonds in different ways. In prions and lysozymes, disulfide bonds keep these proteins from aggregating [2,3]; whereas in human islet amyloid polypeptide (hIAPP), disulfide bond stabilize its α-helix [4], enhancing its aggregation [5,6].

Insulin is a globular protein consisting of two polypeptide chains, the A-chain (21 residues) and the B-chain (30 residues), linked together by two interchain disulfide bonds (A7-B7, A19-B20) and an intrachain disulfide bond (A6-A11) [7]. Each of the three disulfide bonds is required for the structure, stability, receptor binding and biological activity of insulin [8].

Insulin can form fibrils under a range of conditions and this process can be accelerated by impairing native dimerization and the formation of high order self-assemblies [9]. For example, when treated with protein disulfide isomerase (PDI), an enzyme that can break protein disulfide bonds, insulin rapidly aggregated and formed fibrils [10]. The secondary structure of PDI-promoted insulin aggregates are characteristic of anti-parallel β-sheet conformations, revealed by Fourier transform infrared spectroscopy (FT-IR) [10]. In previous studies that investigated how disulfide bonds influence insulin aggregation, reducing reagents like β-mercaptoethanol and dithiothreitol (DTT) were used, with the reduced insulin mixture undergoing aggregation more rapidly than intact insulin [11]. Moreover, we have previously shown that insulin isomers with alternative disulfide pairings [A6-B7, A7-A11, A20-B19] or [A6-A7, A11-B7, A20-B19] readily formed fibrils accompanied with classical α-helix to β-sheet transitions [12].

Despite all this work, the question of how the individual disulfide bonds of insulin affects aggregation remains unanswered. In this work, Tris(2-carboxyethyl)phosphine (TCEP), a mild reducing

Abbreviations: TCEP, Tris(2-carboxyethyl)phosphine; CD, circular dichroism; TEM, transmission electron-microscopy; ThT, Thioflavin-T; PICUP, photo-induced cross-linking of unmodified proteins; RP-HPLC, reversed phase high performance liquid chromatography; Ru(bpy), Tris(2,2'-bipyridyl)dichlororuthenium(II).

* Corresponding authors. Address: Huazhong University of Science and Technology, Tongji School of Pharmacy, Wuhan 430030, PR China. (K. Huang)

E-mail addresses: lzheng217@hotmail.com (L. Zheng), kunhuang2008@hotmail.com (K. Huang).

0006-291X/$ - see front matter © 2012 Elsevier Inc. All rights reserved.
http://dx.doi.org/10.1016/j.bbrc.2012.05.133

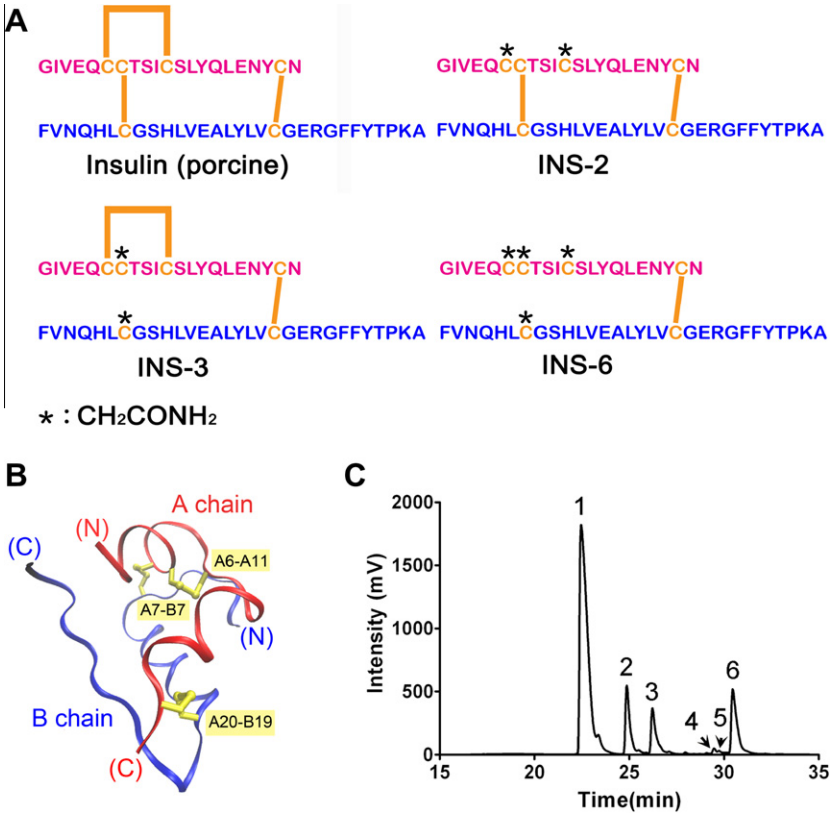

Fig. 1. (A) Primary structure of porcine insulin, INS-2, INS-3 and INS-6. (B) Structural model of porcine insulin (PDB accession number 2EFA), the figure was generated with the program PYMOL. (C) HPLC chromatogram of TCEP partially reduced porcine insulin.

agent, was applied to reduce disulfide bonds in porcine insulin and iodoacetamide was then applied to alkylate partially reduced insulin. In this way, three insulin analogs with separated disulfide bonds, INS-2 (lack of A6-A11), INS-3 (lack of A7-B7) and INS-6 (lack of both A6-A11 and A7-B7), were obtained (Fig. 1A), and their amyloidogenecities were assessed by thioflavin-T (ThT) fluorescence, transmission electronic microscopy (TEM), photo-induced cross-linking of unmodified proteins (PICUP) and hemolysis assays.

2. Materials and methods

2.1. Materials

Porcine insulin (PI) was obtained from Wanbang Biopharmaceuticals (Xuzhou, China). Iodoacetamide, Tris(2-carboxyethyl) phosphine (TCEP), Thioflavin-T (ThT) and Tris(2,2′-bipyridyl) dichlororuthenium(II) (Ru(bpy)) were obtained from Sigma–Aldrich (St. Louis, USA). Fresh blood was drawn from healthy volunteers using heparin as an anticoagulant. All other chemicals were of the highest grade available.

2.2. Sample preparations

2.2.1. Reduction of PI by TCEP

PI was dissolved to a final concentration of 0.5 mg/mL in 100 mM citric buffer (pH 4.5) containing 5% acetonitrile. Freshly prepared TCEP were added to PI solutions to a final concentration of 3.6 mM. The mixtures were incubated at 37 °C for 10 min followed by injecting into a Kromasil C8 semi-preparative reverse-phase column (NY, USA) and monitored at 280 nm. The elution was carried out with a linear gradient of 30–46% acetonitrile for 20 min.

2.2.2. Alkylation of partially reduced PI by iodoacetamide

Iodoacetamide (5 mg) was dissolved in 400 μL Tris–HCl buffer (50 mM, pH 8.5). 0.5 mg of peptide was initially dissolved in 200 μL 0.1% TFA containing 10% acetonitrile and then the peptide solution was diluted into iodoacetamide solution (the molar ratio of iodoacetamine to peptide was 300). The mixture was then kept in dark for 3 min. After alkylation, the peptides were immediately purified by RP-HPLC and lyophilized. Molecular masses were confirmed by matrix-assisted laser desorption ionization (MALDI-TOF) mass spectrometry.

2.3. Far-UV circular dichroism (CD) and data analysis

CD spectra were recorded at 25 °C under a constant flow of N_2 by using a JASCO-810 spectropolarimeter (JASCO, Tokyo, Japan). Data were recorded from 260 to 200 nm with a 1 mm pathlength. Porcine insulin and analogs were dissolved to a final concentration of 20 μM in two solutions: (i) phosphate-buffered saline (PBS, 50 mM phosphate, 100 mM NaCl, pH 7.4); (ii) 0.01 N HCl (0.01 N HCl, 150 mM NaCl, pH 2.0). The spectra were recorded at time intervals resulting from a scanning speed of 50 nm/min, a response time of 1 s and a bandwidth of 2 nm. Each result is given as the average of three measurements. The data were converted to mean residue ellipticity [θ] and were further analyzed using the software package CDPro as described [13].

2.4. Amyloid formation and Thioflavin-T (ThT) fluorescence assays

Insulin and analogs were dissolved in dimethyl sulfoxide (DMSO) and sonicated for 2 min to homogenize samples. Proteins were made to a concentration of 20 μM in each of the following conditions as we previously described [14]: (i) phosphate-buffered saline (PBS, 50 mM phosphate, 100 mM NaCl, pH 7.4); (ii) 0.01 N

HCl (0.01 N HCl, 150 mM NaCl, pH 2.0). All sample solutions contain 0.5% DMSO (control study demonstrated that 0.5% DMSO has no effect on fibrillation, data not shown). Samples at pH 2.0 were incubated at 65 °C and samples prepared in PBS were incubated at 37 °C. All samples were incubated without agitation. Solutions were aliquoted at designated time intervals and thioflavin-T based fluorescence assays were used to detect the formation of amyloid; experiments were performed on a Hitachi FL-2700 fluorometer. The excitation and emission wavelengths were set at 450 nm and 485 nm, respectively. The assay solution contains 50 mM PBS (pH 7.4), 100 mM NaCl and 20 μM thioflavin-T. All experiments were repeated for at least three times. The kinetic curves were calculated as we previously described [14,15].

2.5. Transmission electronic microscopy (TEM)

TEM was performed as we previously described [15]. Briefly, 5 μl of sample was applied onto a 300-mesh Formvar-carbon coated copper grid (Shanghai, China) followed by staining with 1% fresh prepared uranyl formate. Samples were air dried and observed under a transmission microscope (Hitachi, Tokyo, Japan) operating at an accelerating voltage of 150 kV.

2.6. Photo-induced cross-linking of unmodified proteins (PICUP) assay

Insulin and its analogs were dissolved in 1% acetic acid solution to a final concentration of 50 μM and sonicated for 2 min to homogenize. Samples were photo-crosslinked using the PICUP method [16,17]. The reaction buffer consists of 200 μM Ru(bpy), 400 μM ammonium persulfate and 10 μM proteins. The mixture was irradiated for 5 s with a 150 W incandescent lamp installed in a house-made dark-box. After irradiation, 5 μl loading buffer was immediately added, followed by denaturation at 97 °C for 10 min. The cross-linked samples were separated on a 20% Tricine-Urea gel and visualized by a fast silver stain kit (Beyotime, Jiangsu, China).

2.7. Hemolysis assay

Hemolysis assays were performed as described [18]. Fresh blood was centrifuged at 1000*g* for 10 min, and erythrocytes were separated from plasma and washed three times with isotonic phosphate buffered saline (pH 7.4). For hemolytic assay, cell suspensions (1% hematocrit) were incubated at 37 °C for 24 h in the presence of insulin or analogs. An aliquot of the reaction mixture was removed and centrifuged at 1000*g* for 10 min. Absorbance of the supernatant was determined at 540 nm. The hemolytic rate was calculated in relation to the hemolysis of erythrocytes in 10 mM phosphate buffer, which was taken as 100%.

2.8. Statistical analysis

All results were expressed as the mean ± SD. To evaluate statistical significance, data variance was analyzed with the Kruskal–Wallis test, followed by the Mann–Whitney test. Difference was considered statistically significant at $P < 0.05$.

3. Results

3.1. Reduction and alkylation of insulin

Mild reduction of insulin was carried out at pH 4.5, under which TCEP has a relative low activity that enables a gradual reduction of three disulfide bonds in insulin instead of an unwanted simultaneous reduction of all three bonds, which would separate insulin into two peptide chains. After incubating for 10 min, the reduced products were analyzed by RP-HPLC. There were six main peaks (Fig. 1C) in the chromatograph, in addition to insulin (peak 1), five new peaks appeared (designated INS-2∗ - INS-6∗, Fig. 1C). All peaks were collected and their molecular masses were measured by MALDI-TOF MS (Supplementary Table S1). Based on MS results and a previous report [19], INS-2∗ was identified as an analog with disulfide A6-A11 reduced, INS-3∗ had reduced A7-B7, and INS-6∗ had both A6-A11 and A7-B7 reduced. INS-4∗and INS-5∗ were insulin B chain and A chain, respectively.

Free thiol groups can be easily oxidized by atmospheric oxygen to form native or exchanged disulfide bonds. To protect the free thiols in INS-2∗, INS-3∗ and INS-6∗ from oxidization, alkylation was performed followed by RP-HPLC purification (Supplementary Fig. S1). Products were collected and lyophilized. Three stable alkylated insulin analogs, INS-2, INS-3 and INS-6 (Fig. 1A), were obtained and their molecular masses were confirmed by MALDI-TOF MS (Supplementary Table S1).

3.2. Influence of disulfide deletion on secondary structures

The secondary structures of analogs were analyzed by far-UV CD spectroscopy. In the far-UV region, the spectra of the three analogs are significantly different from that of insulin, showing less ordered secondary structures (Fig. 2). Deconvolution results indicated that insulin has 42.0% α-helical content at pH 7.4, a result in close agreement with the crystal structure. Whereas the three analogs exhibited significantly decreased α-helix contents compared to the native molecule (INS-2, 30.1%; INS-3, 28.4%; and INS-6, 14.5% (Supplementary Table S2)). At pH 2.0, the α-helix content of insulin increased to 56.8% whereas all analogs showed decreased α-helix contents and increased β structures (Fig. 2B and Supplementary Table S2).

3.3. Influence of disulfide bonds on the amyloidogenecity of insulin

To investigate how disulfide breakage may affect the amyloidogenecity of insulin, ThT-based fluorescence was performed to monitor the kinetics of amyloid formation. Insulin and all analogs readily form amyloids at pH 2.0 and 65 °C, however, the fibrillation processes of all the analogs were markedly accelerated. Compared to insulin (8.12 ± 0.19 h), INS-6 has the shortest lag time of 0.55 ± 0.03 h, followed by INS-3 (2.31 ± 0.09 h) and INS-2 (4.68 ± 0.20 h) (Fig. 3A and Table 1). At pH 7.4 and 37 °C, a similar trend was also observed (Fig. 3B and Tale 1).

The morphologies of fibrils of insulin and its analogs were observed by TEM. Insulin and analogs formed meshes of typical long linear fibrils at pH 2.0 and 65 °C after 12 h incubation (Fig. 3C–F). Under neutral conditions, no obvious insulin fibrils were observed after incubating for 4 days without agitation (Fig. 3G), whereas INS-2 and INS-6 formed typical long linear fibrils (Fig. 3H and J), and INS-3 formed precipitate-like aggregates (Fig. 3I).

3.4. Hemolysis of erythrocytes induced by oligomers and fibrils of samples

Previous studies demonstrated that insulin oligomers and fibrils can cause hemolysis of erythrocytes by disrupting cell membranes [18]. In this study, erythrocytes were incubated with insulin and the three analogs for 24 h in an isotonic environment. The level of hemolysis of erythrocytes was 30.8 ± 3.3% for control cells and no significant changes were found in erythrocytes treated with insulin (32.3 ± 2.2%, $p = 0.490$) and INS-3 (35.1 ± 2.3%, $p = 0.136$), respectively (Fig. 4A). For erythrocytes treated with INS-2 and INS-6, the levels of hemolysis raised to 50.2 ± 8.9 ($p < 0.05$) and 55.2 ± 7.1 ($p < 0.05$), respectively (Fig. 4A).

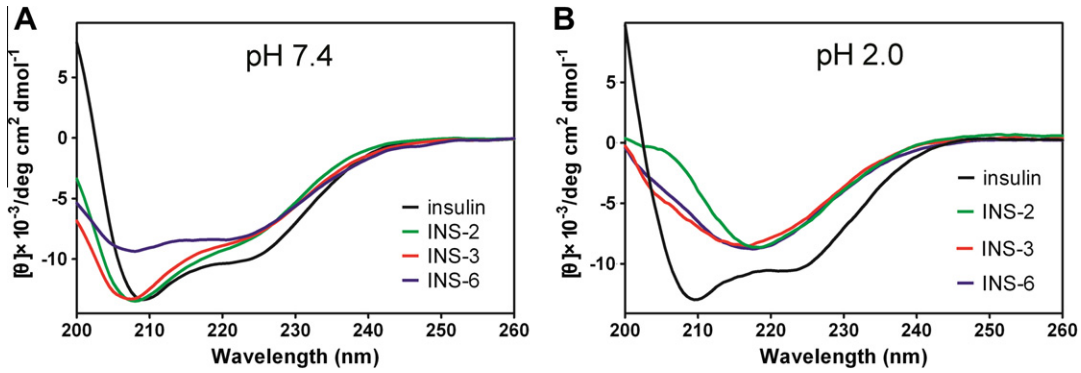

Fig. 2. Far-UV circular dichroism spectra of porcine insulin, INS-2, INS-3 and INS-6 dissolved in (A) phosphate-buffered saline (PBS, 50 mM phosphate, 100 mM NaCl, pH 7.4); (B) 0.01 N HCl (0.01 N HCl, 150 mM NaCl, pH 2.0) .

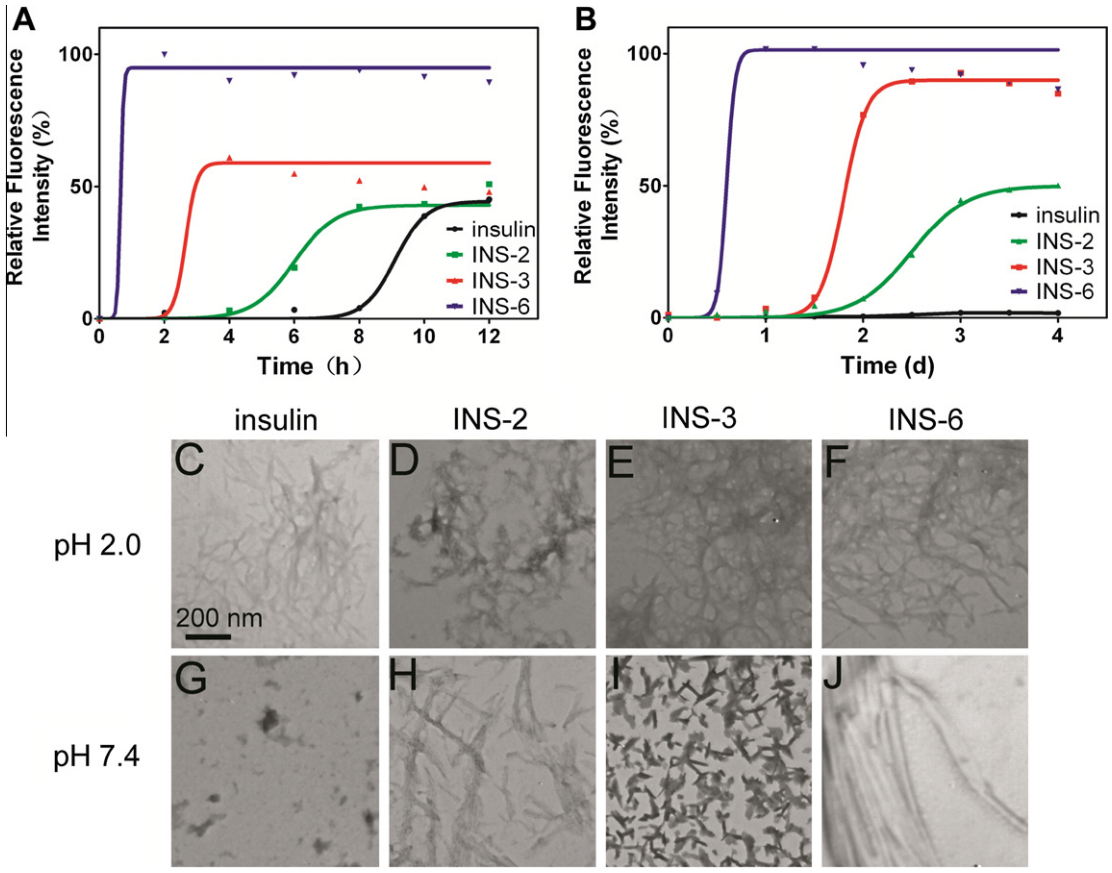

Fig. 3. Amyloidogenecity of insulin and analogs. (A and B) Relative thioflavin-T fluorescence intensity of insulin and analogs incubated at (A) pH 2.0, 65 °C and (B) pH 7.4, 37 °C without agitation. (C–J) TEM morphologies of insulin and its analogs fibrils under (C–F) acid and (G–J) neutral conditions.

Table 1
List of lag times of insulin and its analogs.[a].

Proteins[b]	pH 2.0		pH 7.4	
	Lag time (h)	Intensity (%)[c]	Lag time (days)	Intensity (%)[c]
Porcine insulin	8.12 ± 0.19	48.6 ± 7.0	N[d]	9.3 ± 3.7
INS-2	4.68 ± 0.20	47.5 ± 4.5	1.99 ± 0.13	48.7 ± 5.2
INS-3	2.31 ± 0.09	64.4 ± 8.0	1.51 ± 0.06	65.2 ± 7.6
INS-6	0.55 ± 0.03	100.0 ± 3.9	0.52 ± 0.04	100.0 ± 7.2

[a] All assays were repeated for at least three times.
[b] The concentration of proteins was 20 μM.
[c] The fluorescence intensity of INS-6 was set as 100.
[d] N, the lag time and t_{50} were too long to be accurately calculated during the test.

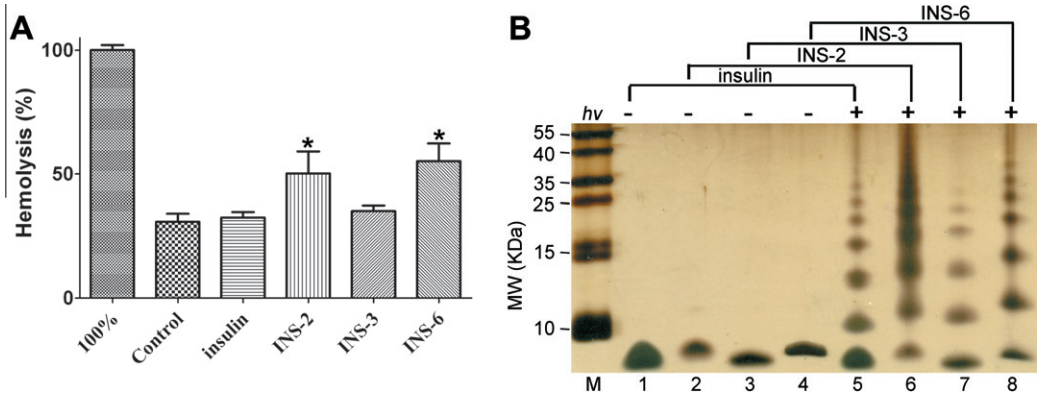

Fig. 4. (A) Hemolysis of erythrocytes induced by insulin and its analogs after 24 h incubation. Hypotonic solution treated erythrocytes were used as 100% and untreated were used as controls. $^{*}p < 0.05$. (B) Oligomerization status of samples studied by the photo-induced cross linking assays. Lanes 1–4, insulin, INS-2, INS-3 and INS-6 without irradiation; lanes 5–8, insulin, INS-2, INS-3 and INS-6 irradiated for 5 s.

3.5. Oligomerization studied by PICUP

The influence of disulfide bonds on oligomerization was determined with the PICUP-based photo-cross-linking method. Without irradiation, insulin and analogs migrated mostly as a monomer (lanes 1–4, Fig. 4B); after a short period of light exposure (5 s), extensive oligomerization was detected, consisting of monomer, dimer, trimer, tetramer, and higher oligomers (lanes 5–8, Fig. 4B). Unlike INS-6 and INS-2, INS-3 formed almost no oligomers above 35 KDa, indicating a slower oligermerization process.

4. Discussion

In this study, we found insulin analogs that have disulfide bonds A6-A11 and/or A7-B7 reduced can be readily obtained with our protocols. However, among a variety of reducing conditions tested, no analog with the A20-B19 being reduced was obtained, which is reasonable since A20-B19 has been reported as the foremost formed disulfide bond during the folding of proinsulin [20], and is also the most buried (the least accessible) disulfide bond of the three, stabilizing the entire molecule [21]. This makes A20-B19 the last disulfide bond that is accessible to TCEP, suggesting that the breakage of A20-B19 must take place after the reduction of the other two disulfide bonds. Therefore the breakage of A20-B19 results in the seperation of insulin into A and B chains [19], which were observed at very low levels by RP-HPLC (Fig. 1B).

Far-UV CD spectroscopy results indicated that at a neutral pH, the interchain disulfide A7-B7 plays a more important role on the structure of insulin than the intrachain disulfide A6-A11 (Fig. 2A and Supplementary Table S2). In previous reports, deletion of A6-A11 induced unfolding of α-helices (A2–A8) [22,23], whereas the deletion of A7-B7 induced the unfolding of both α-helix A2–A8 and a portion of A13–A19 [24], which is consistent with our CD results (Fig. 2). In a previous study, an insulin analog with A20-B19 deleted has no detectable helical content [25]. In contrast, analog INS-6, which only retains A20-B19, still has 14% α-helical content (Supplementary Table S2). These results provide further evidence that A20-B19 plays a central role on the structure of insulin that cannot be replaced by the other disulfide bonds. On the other hand, at the acidic pH of 2.0, all analogs significantly lost their α-helical content accompanied with an increased β-structure.

For amyloidogenecity, ThT fluorescence results showed all analogs formed fibrils more rapidly than insulin, and INS-3 has shorter lag phases than INS-2 under both tested conditions (Fig. 3A, B and Table 1). These results indicated that the breakage of either disulfide bonds accelerates fibrillation, and that this acceleration was more prominent with the breakage of the interchain disulfide A7-B7. The protein fibrillation can be affected by the exposure of its hydrophobic groups [26]; in a globular protein like native insulin, the hydrophobic residues are largely buried to form a hydrophobic core [26], reduction of its disulfide bonds partially unfolds the molecule (Fig. 2) and exposes its hydrophobic surfaces, which results in accelerated formation of amyloid fibrils.

It was interesting to note that the single deletion of disulfide A7-B7 did not cause significant cytotoxicity as the hemolysis results suggested (Fig. 4), which seem to be inconsistent with the ThT-assay results. A plausible explanation is that as it is generally accepted that the species that are highly toxic to cells are the prefibrillar aggregates (high order oligomers; [27]), which can impair cell function by interacting with cell membranes, causing oxidative stress and the level of free calcium ions to increase, eventually leading to apoptotic or necrotic cell death [28]. In our PICUP assays, we demonstrated that INS-3 had a lower potential to form oligomers (Fig. 4B), which raises the possibility that the oligomers of INS-3 are less stable compared to those of the other analogs, which is consistent with the reduced cytotoxicity of INS-3.

In summary, in this study, three insulin analogs with partially reduced disulfide bonds were obtained by controlled reduction and alkylation. Compared to the intrachain disulfide A6-A11, breakage of the interchain disulfide A7-B7 disrupts the insulin structure more significantly and was accompanied with even higher amyloidogenecity. On the other hand, breakage of disulfide A6-A11 is associated with significantly increased cytotoxicity that may resulted from a higher potency to form high order cytotoxic oligomers.

Acknowledgments

This work was supported by the National Basic Research Program of China (2009BC918304 and 2012CB524901), the Natural Science Foundation of China (Nos. 30801445, 30970607 and 81172971), and the Program for New Century Excellent Talents in University (NECT10-0623 and NECT11-0170). The authors are grateful to the Analytical and Testing Center of Huazhong University of Science and Technology, and Research Core Facility of College of Life Sciences, Wuhan University for analytical supports. The authors wish to thank Mr. Mitchell Sullivan (University of Queensland) for editing the manuscript.

Appendix A. Supplementary data

Supplementary data associated with this article can be found, in the online version, at http://dx.doi.org/10.1016/j.bbrc.2012.05.133.

References

[1] C.M. Dobson, Protein folding and its links with human disease, Biochem. Soc. Symp. (2001) 1–26.
[2] I. Mehlhorn, D. Groth, J. Stockel, B. Moffat, D. Reilly, D. Yansura, W.S. Willett, M. Baldwin, R. Fletterick, F.E. Cohen, R. Vandlen, D. Henner, S.B. Prusiner, High-level expression and characterization of a purified 142-residue polypeptide of the prion protein, Biochemistry 35 (1996) 5528–5537.
[3] A. Cao, D. Hu, L. Lai, Formation of amyloid fibrils from fully reduced hen egg white lysozyme, Protein Sci. 13 (2004) 319–324.
[4] I.T. Yonemoto, G.J. Kroon, H.J. Dyson, W.E. Balch, J.W. Kelly, Amylin proprotein processing generates progressively more amyloidogenic peptides that initially sample the helical state, Biochemistry 47 (2008) 9900–9910.
[5] M. Apostolidou, S.A. Jayasinghe, R. Langen, Structure of alpha-helical membrane-bound human islet amyloid polypeptide and its implications for membrane-mediated misfolding, J. Biol. Chem. 283 (2008) 17205–17210.
[6] J.T. Nielsen, M. Bjerring, M.D. Jeppesen, R.O. Pedersen, J.M. Pedersen, K.L. Hein, T. Vosegaard, T. Skrydstrup, D.E. Otzen, N.C. Nielsen, Unique identification of supramolecular structures in amyloid fibrils by solid-state NMR spectroscopy, Angew. Chem., Int. Ed. Engl. 48 (2009) 2118–2121.
[7] T.L. Blundell, J.F. Cutfield, S.M. Cutfield, E.J. Dodson, G.G. Dodson, D.C. Hodgkin, D.A. Mercola, Three-dimensional atomic structure of insulin and its relationship to activity, Diabetes 21 (1972) 492–505.
[8] Q.X. Hua, J.P. Mayer, W. Jia, J. Zhang, M.A. Weiss, The folding nucleus of the insulin superfamily: a flexible peptide model foreshadows the native state, J. Biol. Chem. 281 (2006) 28131–28142.
[9] L. Nielsen, R. Khurana, A. Coats, S. Frokjaer, J. Brange, S. Vyas, V.N. Uversky, A.L. Fink, Effect of environmental factors on the kinetics of insulin fibril formation: elucidation of the molecular mechanism, Biochemistry 40 (2001) 6036–6046.
[10] R. Maeda, K. Ado, N. Takeda, Y. Taniguchi, Promotion of insulin aggregation by protein disulfide isomerase, Biochim. Biophys. Acta 1774 (2007) 1619–1627.
[11] D. Givol, F. Delorenzo, R.F. Goldberger, C.B. Anfinsen, Disulfide interchange and the three-dimensional structure of proteins, Proc. Natl. Acad. Sci. USA 53 (1965) 676–684.
[12] K. Huang, N.C. Maiti, N.B. Phillips, P.R. Carey, M.A. Weiss, Structure-specific effects of protein topology on cross-beta assembly: studies of insulin fibrillation, Biochemistry 45 (2006) 10278–10293.
[13] N. Sreerama, R.W. Woody, Computation and analysis of protein circular dichroism spectra, Methods Enzymol. 383 (2004) 318–351.
[14] K. Huang, J. Dong, N.B. Phillips, P.R. Carey, M.A. Weiss, Proinsulin is refractory to protein fibrillation: topological protection of a precursor protein from cross-beta assembly, J. Biol. Chem. 280 (2005) 42345–42355.
[15] X. Zhang, B. Cheng, H. Gong, C. Li, H. Chen, L. Zheng, K. Huang, Porcine islet amyloid polypeptide fragments are refractory to amyloid formation, FEBS Lett. 585 (2011) 71–77.
[16] G. Bitan, D.B. Teplow, Rapid photochemical cross-linking–a new tool for studies of metastable, amyloidogenic protein assemblies, Acc. Chem. Res. 37 (2004) 357–364.
[17] B. Cheng, X. Liu, H. Gong, L. Huang, H. Chen, X. Zhang, C. Li, M. Yang, B. Ma, L. Jiao, L. Zheng, K. Huang, Coffee components inhibit amyloid formation of human islet amyloid polypeptide in vitro: possible link between coffee consumption and diabetes mellitus, J. Agric. Food Chem. 59 (2011) 13147–13155.
[18] J.B. Wang, Y.M. Wang, C.M. Zeng, Quercetin inhibits amyloid fibrillation of bovine insulin and destabilizes preformed fibrils, Biochem. Biophys. Res. Commun. 415 (2011) 675–679.
[19] W.R. Gray, Disulfide structures of highly bridged peptides: a new strategy for analysis, Protein Sci. 2 (1993) 1732–1748.
[20] X.Y. Jia, Z.Y. Guo, Y. Wang, Y. Xu, S.S. Duan, Y.M. Feng, Peptide models of four possible insulin folding intermediates with two disulfides, Protein Sci. 12 (2003) 2412–2419.
[21] Q. Hua, Insulin: a small protein with a long journey, Protein Cell 1 (2010) 537–551.
[22] Q.X. Hua, S.Q. Hu, B.H. Frank, W. Jia, Y.C. Chu, S.H. Wang, G.T. Burke, P.G. Katsoyannis, M.A. Weiss, Mapping the functional surface of insulin by design: structure and function of a novel A-chain analogue, J. Mol. Biol. 264 (1996) 390–403.
[23] M.A. Weiss, Q.X. Hua, W. Jia, Y.C. Chu, R.Y. Wang, P.G. Katsoyannis, Hierarchical protein "un-design": insulin's intrachain disulfide bridge tethers a recognition alpha-helix, Biochemistry 39 (2000) 15429–15440.
[24] Q.X. Hua, S.H. Nakagawa, W. Jia, S.Q. Hu, Y.C. Chu, P.G. Katsoyannis, M.A. Weiss, Hierarchical protein folding: asymmetric unfolding of an insulin analogue lacking the A7–B7 interchain disulfide bridge, Biochemistry 40 (2001) 12299–12311.
[25] S.G. Chang, K.D. Choi, S.H. Jang, H.C. Shin, Role of disulfide bonds in the structure and activity of human insulin, Mol. Cells 16 (2003) 323–330.
[26] C.M. Dobson, Protein folding and misfolding, Nature 426 (2003) 884–890.
[27] M. Bucciantini, E. Giannoni, F. Chiti, F. Baroni, L. Formigli, J. Zurdo, N. Taddei, G. Ramponi, C.M. Dobson, M. Stefani, Inherent toxicity of aggregates implies a common mechanism for protein misfolding diseases, Nature 416 (2002) 507–511.
[28] M. Stefani, C.M. Dobson, Protein aggregation and aggregate toxicity: new insights into protein folding, misfolding diseases and biological evolution, J. Mol. Med. (Berl) 81 (2003) 678–699.